b-flavour tagging in *pp* collisions

Alex Birnkraut[*]

TU Dortmund

E-mail: a.birnkraut@cern.ch

In the system of neutral *B* mesons *CP*-violation and neutral meson mixing can be measured using time-dependent analyses, as performed at the LHCb experiment. For such analyses the knowledge of the flavour of the mesons at production is mandatory. This information is provided by "flavour tagging" techniques. A description of the flavour tagging algorithms used at the LHCb experiment during Run I for *pp* collisions at $\sqrt{s} = 7, 8\,\text{TeV}$ is reported. The good performance of the flavour tagging techniques allow high precision measurements in the B^0 and B_s^0 sector. Some recent developments are also discussed.

The European Physical Society Conference on High Energy Physics
22–29 July 2015
Vienna, Austria

---

[*]Speaker.

1. Introduction

The aim of the Flavour Tagging algorithms is to determine the flavour of neutral B mesons at their production. These algorithms are called taggers and can be classified in two groups. The same side (SS) taggers use charged particles which are created in the fragmentation process of the signal b quark. The opposite side (OS) taggers infer the flavour of the non-signal b quark of the $b\bar{b}$ pair produced in the pp collision by looking e.g. for leptons originating from semileptonic $b \to cW$ transitions or kaons coming from $b \to c \to s$ transitions (Figure 1) [1].

The performance of the Flavour Tagging algorithms is characterised with the tagging efficiency

$$\varepsilon_{\text{tag}} = \frac{N_{\text{right}} + N_{\text{wrong}}}{N_{\text{all}}}, \tag{1.1}$$

the probability of the tagging decision to be wrong

$$\omega = \frac{N_{\text{wrong}}}{N_{\text{right}} + N_{\text{wrong}}} \tag{1.2}$$

and the dilution $D = 1 - 2\omega$. The quantities N_{right}, N_{wrong} and N_{all} are the numbers of the right taged, wrong tagged and all candidates respectively, i.e. tagged and untagged candidates.

Each tagger provides a per-event tag decision d and a probability η to be wrong. This predicted mistag probability η is calibrated on data with a function $\omega(\eta)$. Weighting each signal candidate with $D = 1 - 2\omega(\eta)$ leads to an corrected per-event dilution factor. The statistical power of a CP or mixing asymmetry measurement using tagging algorithms is proportional to an effective tagging efficiency

$$\varepsilon_{\text{eff}} = \varepsilon_{\text{tag}} \left(1 - 2\omega(\eta)\right). \tag{1.3}$$

Thus any augmentation to this effective tagging efficiency increases the statistical precision in these time dependent measurements at LHCb.
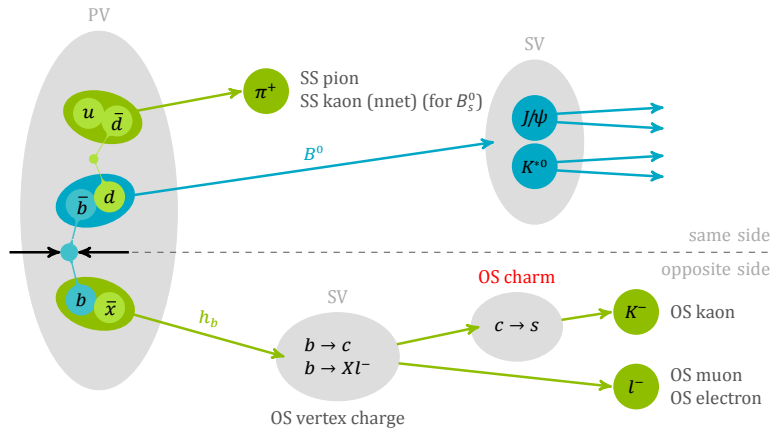

Figure 1: Scheme of the different flavour tagging algorithms. Same side taggers are shown in the upper part, opposite side taggers in the lower part.

2. Flavour Tagging algorithms at LHCb

For the opposite side tagging algorithms there are mainly two different types of algorithms. Single particle taggers identify electrons, muons and kaons coming from the other *b* hadron. To select these particles a large impact parameter significance with respect to the primary vertex and a large transverse momentum p_T are required. For particle identification cuts on the difference between the logarithm of the likelihood for the muon, electron, kaon or proton and the pion hypothesis are applied. In case of multiple candidates from one tagging algorithm the candidate with the highest transverse momentum is chosen.

In contrast to this method the OS vertex charge tagger does not use single tracks but a weighted charge of a secondary vertex to take a tag decision. The secondary vertex is reconstructed from two tracks which have the highest probablity to originate from the OS *b* hadron. From this seed more tracks that are compatible with coming from the secondary vertex but not from the primary vertex are added to the vertex to form the final *b*hadron candidate. Finally a weighted charge is calculated as a sum of the charges Q_i of all tracks associated to the vertex

$$Q_{\text{vtx}} = \frac{\sum_i p_T^k(i) Q_i}{\sum_i p_T^k(i)},$$ (2.1)

weighted by their transverse momentum p_T to the power k. The value k optimises the effective tagging efficiency.

For the same side tagging one has to distinguish between B_d^0 and B_s^0 mesons as the accompanying quark is a *d* or a *s* quark, respectively. In case of a B_d^0 meson an additional pion from the *d* quark which can hadronise with an *u* quark emerges. Also pions from excited states as B^* and B^{**} have the same charge as pions from the direct fragmenation process with a B^0 meson. Therefore the pion candidates are required to be charged particles with high momentum and transverse momentum originating from the primary vertex [10]. If the signal *B* meson is a B_s^0 a kaon can be formed out of the additional *s* quark and an *u* quark.

For each tagger a multivariate classifier trained on simulated data distinguishes between correct and incorrect tag decisions *d*. For each decision made, this classifier then calculates the mistag probablity η. Inputs to this classifier

2.1 SS kaon tagging using neural nets (NN)

The first version of the SS kaon tagger uses a selection based on rectangular cuts to identify the tagging kaon and a neural net (NN) was only used to estimate the mistag probabilty η. For the SS kaon neural net tagger the basic idea is to use two NN. The first NN distinguishes between fragmentation tracks and the underlying event tracks (see figure 2.1). The fragmentation tracks are the signal tracks for the SS kaon tagger, i.e. the tracks are the searched tagging particle tracks [2]. The second NN assigns the final tag and mistag based on multiple candidates [3].

Compared to the cut-based SS kaon the SS kaon NN gives a relative improvement of 50 % (41 %) in ε_{eff} for $B_s^0 \to D_s^- \pi^+$ ($B_s^0 \to J/\psi\phi$). This improvements can be observed also when comparing the effective tagging efficiencies in the measurements of ϕ_s at LHCb. The effective tagging efficiencies ε_{eff} for the *CP* analyses in $B_s^0 \to J/\psi K^+ K^-$, $\bar{B}_s^0 \to J/\psi\pi^+\pi^-$ and $\bar{B}_s^0 \to D_s^+ D_s^-$ are listed in table 2.1.
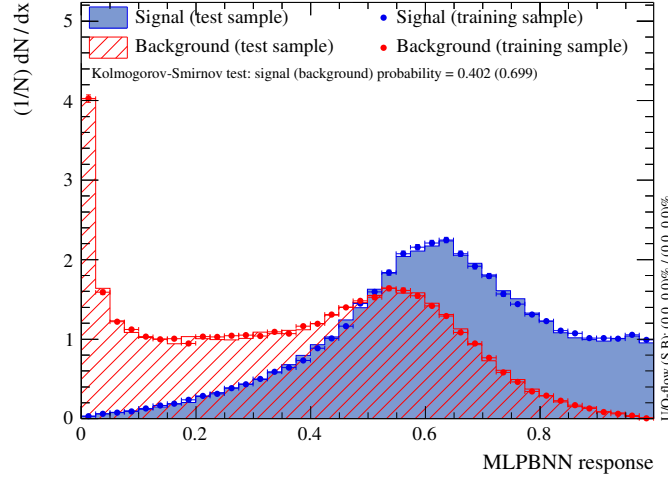
Figure 2: Distribution of NN response for fragmentation tracks (signal) and underlying event tracks (background) [2]

Decay mode	ε_{eff} (1 fb^{-1})	ε_{eff} (3 fb^{-1})
$B_s^0 \rightarrow J/\psi K^+ K^-$	3.13 % [4]	3.73 % [5]
$\bar{B}_s^0 \rightarrow J/\psi \pi^+ \pi^-$	2.43 % [6]	3.89 % [7]
$\bar{B}_s^0 \rightarrow D_s^+ D_s^-$	-	5.33 % [8]

Table 1: Tagging efficiencies and effective tagging efficiencies for the *CP* analyses measuring ϕ_s. In the analyses on 1 fb^{-1} the cut-based version of the SS kaon was used, the analyses on the whole Run I dataset with 3 fb^{-1} used the neural net based version.

2.2 OS charm tagger

The OS charm tagger uses charm hadrons from the decay chain $b \rightarrow c$ from the opposite side b quark to tag the initial flavour. The reconstructed D modes related to the OS b decay are listed in table 2.2. For each mode one boosted decision tree is used to calculate the mistag probybility η and then the candidate with the best prediction is picked [11]. The OS charm tagger provides a relatively clean measure of the B flavour, i.e. it provides low values of η. Depending on the decay mode its stand-alone effective tagging efficiency is $\varepsilon_{\text{eff}} = 0.30\%$ to 0.40%.

3. Calibration of the Flavour Tagging

The mistag estimate η provided by the different tagging algorithms has to be corrected and transformed into the true mistag probabilty ω. This is done with a linear calibration function

$$\omega(\eta) = p_0 + p_1 (\eta - \langle \eta \rangle) \tag{3.1}$$

with the mean mistag estimate $\langle \eta \rangle$. The parameters p_0 and p_1 of this calibration function are extracted in to different ways. Using charged decay modes as $B^+ \rightarrow J/\psi K^+$ and $B^+ \rightarrow D^0 \pi^+$ the true mistag ω can be extracted by comparing the tag with the charge of the kaon or pion in

Decay mode	Relative ε_{tag}	Relative ε_{eff}
$D^0 \to K^- \pi^+$	10.0 %	24.0 %
$D^0 \to K^- \pi^+ \pi^+ \pi^-$	5.9 %	8.4 %
$D^+ \to K^- \pi^+ \pi^+$	10.3 %	2.6 %
$D^0, D^+ \to K^- \pi^+ X$	69.7 %	61.5 %
$D^0, D^+ \to K^- e^+ X$	0.5 %	0.2 %
$D^0, D^+ \to K^- \mu^+ X$	3.4 %	0.3 %
$\Lambda_c^+ \to p^+ K^- \pi^+$	0.2 %	2.4 %

Table 2: D meson decay modes with their relative contributions to ε_{tag} and ε_{eff} which are used by the OS charm tagger.

the final state. In neutral decay modes as $B^0 \to J/\psi K^{*0}$, $B^0 \to D^{*-} \mu^+ \nu_\mu$ or $B_s^0 \to D_s^- \pi^+$ a full time-dependent analysis is needed to extract omega from the mixing asymmetry:

$$A_{\text{mix}}(t) \propto (1 - 2\omega) \cos \left(\Delta m_{d/s} t \right) \tag{3.2}$$

In both cases the calculation of ω is done in bins of the mistag estimate η and the linear function 3.1 is fitted to the (ω, η) pairs. Figure 3 shows for one bin the time dependent mixing asymmetry and the linear calibration function for the calibration mode $B^0 \to J/\psi K^{*0}$.
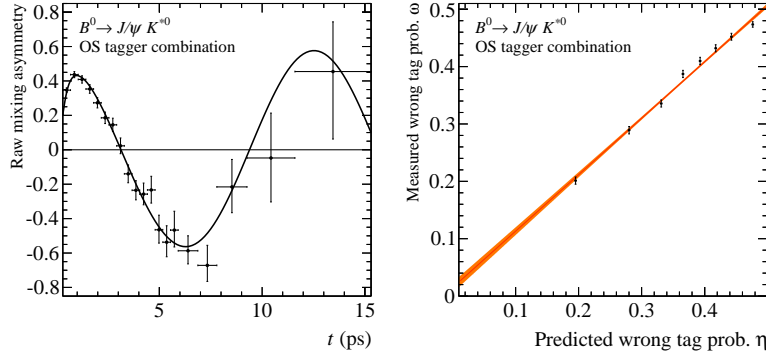

Figure 3: Mixing asymmetry (left) and calibration function (right) for the OS tagger combination in the calibration mode $B^0 \to J/\psi K^{*0}$.

3.1 Flavour Tagging in Run I

For most of the analyses performed during Run I the uncertainties which came from the Flavour Tagging calibration were much smaller than the statistical uncertainties. Therefore one calibration per tagger valid for all channels was provided. The systematic uncertainties were calculated due to direct uncertainties on the calibration and the results from different control channels, which were used for the calibration. The direct uncertainties on the calibration are e.g. influences of the fit model of the mass to separete signal and background candidates.

For analyses where the uncertainties were dominated by the Flavour Tagging uncertainties an "ad-hoc" calibration using the best-suited control channel for the analyses was performed.
In the following some recent developments in the Flavour Tagging are presented.

3.2 *CP* violation in $B^0 \to J/\psi K_s^0$ ($\sin 2\beta$)

The measurement of *CP* violation in $B^0 \to J/\psi K_s^0$ was performed both on $1\,\mathrm{fb}^{-1}$ and on the whole Run I dataset of $3\,\mathrm{fb}^{-1}$. The effective tagging power increased from $\varepsilon = 2.38\,\%$ ($1\,\mathrm{fb}^{-1}$) [9] to $\varepsilon = 3.02\,\%$ ($3\,\mathrm{fb}^{-1}$) [10]. This increase was due to the usage of the SS pion tagger which adds more than $0.376\,\%$ in the newest analysis. As the measurement of $\sin 2\beta$ is a precision analysis an "ad-hoc" calibration was performed. The OS taggers were calibrated with the control channel $B^+ \to J/\psi K^+$, the SS pion tagger was calibrated with $B^0 \to J/\psi K^{*0}$. For both modes systematic uncertainties were evaluated on the calibration method itself and due to the portability to the $B^0 \to J/\psi K_s^0$ decay.

4. Conclusion

During Run I the performance of the Flavour Tagging improved for the SS kaon tagging and for the OS tagging in the order of $40\,\%$ and $15\,\%$ respectively. Many time-dependent measurements could be performed successfully with high precision and new developments as the OS kaon NN tagging were established.

References

[1] LHCb Collaboration, R.Aaij et. al., *Opposite-side flavour tagging of B mesons at the LHCb experiment, Eur.Phys.J.* C72 (2012) 2022

[2] LHCb Collaboration, R. Aaij et. al., *Optimization and calibration of the same-side kaon tagging algorithm using hadronic B_s^0 decays in 2011 data,* LHCb-CONF-2012-033

[3] G. A. Krocker, *Development and calibration of a same side kaon tagging algorithm and measurement of the $B_s^0 - \bar{B}_s^0$ oscillation frequency Δm_s at the LHCb experiment,* PhD thesis, Heidelberg U., Sep, 2013, CERN-THESIS-2013-213

[4] LHCb Collaboration, R. Aaij et. al., *Measurement of CP violation and the B_s^0 meson decay width difference with $B_s^0 \to J/\psi K^+ K^-$ and $\bar{B}_s^0 \to J/\psi \pi^+ \pi^-$ decays,* Phys.Rev. D87 (2013) 11, 112010

[5] LHCb Collaboration, R. Aaij et. al., *Precision measurement of CP violation in $B_s^0 \to J/\psi K^+ K^-$ decays,* Phys.Rev.Lett. 114 (2015) 4, 041801

[6] LHCb Collaboration, R. Aaij et. al., *Measurement of the CP-violating phase ϕ_s in $\bar{B}_s^0 \to J/\psi \pi^+ \pi^-$ decays,* Phys.Lett. B713 (2012) 378-386

[7] LHCb Collaboration, R. Aaij et. al., *Measurement of the CP-violating phase ϕ_s in $\bar{B}_s^0 \to J/\psi \pi^+ \pi^-$ decays,* Phys.Lett. B736 (2014) 186-195

[8] LHCb Collaboration, R. Aaij et. al., *Measurement of the CP-violating phase ϕ_s in $\bar{B}_s^0 \to D_s^+ D_s^-$ decays,* Phys.Rev.Lett. 113 (2014) 21, 211801

[9] LHCb Collaboration, R. Aaij et. al., *Measurement of the time-dependent CP asymmetry in $B^0 \to J/\psi K_s^0$ decays,* Phys.Lett. B721 (2013) 24-31

[10] LHCb Collaboration, R. Aaij et. al., *Measurement of CP violation in $B^0 \to J/\psi K_s^0$ decays,* Phys.Rev.Lett. 115 (2015) 3, 031601

[11] LHCb Collaboration, R. Aaij et. al., *B flavor tagging using reconstructed charm decays at the LHCb experiment,* LHCb-PAPER-2015.027